SLAC-PUB-6695
October 1994
T/E

THE CHARM PHYSICS POTENTIAL OF A TAU-CHARM FACTORY*†

J.L. HEWETT
Stanford Linear Accelerator Center, Stanford University, Stanford, CA 94309

ABSTRACT

The charm physics program accessible to a Tau-Charm Factory is summarized. Semileptonic, leptonic, hadronic, rare and forbidden charm decay modes are discussed, as well as $D^0 - \bar{D}^0$ mixing and CP violation in the charm sector. The theoretical expectations in the Standard Model and beyond as well as the experimental capabilities of a Tau-Charm Factory are examined for each of the above processes.

1. Overview

One of the outstanding problems in particle physics is the origin of the fermion mass and mixing spectrum. At present the best approach in addressing this question is to study the properties of all heavy fermions in detail. While investigations of the K and B systems have and will continue to play a central role in the quest to understand flavor physics, in-depth examinations of the charm-quark sector have yet to be performed, leaving a gap in our knowledge. Since charm is the only heavy charged $+2/3$ quark presently accessible to experiment, it provides the sole window of opportunity to examine flavor physics in this sector. In addition, charm allows a complimentary probe of Standard Model (SM) physics (and beyond) to that attainable from the down-quark sector.

Detailed measurements of heavy quark systems are best realized at high precision, high luminosity machines. Here we discuss the charm physics potential at a high luminosity ($\mathcal{L} = 10^{33}$ cm^{-2} sec^{-1}) e^+e^- collider operating at the $c\bar{c}$ and $\tau\bar{\tau}$ threshold region, *i.e.*, a Tau-Charm Factory (τcF). Such a machine would facilitate an in-depth analysis of the charm-quark sector (as well as τ-lepton[1] and charmonium[2] studies) without the contamination of b-quark production. The high luminosity is absolutely essential in order to accomplish the physics goals of the machine. In some cases it is necessary in order to measure a reaction at the high level of precision that is desired, while in other cases, high luminosity is required to reach the very small transition rates.

*Work supported by the Department of Energy, Contract DE-AC03-76SF00515

†To appear in *The Tau-Charm Factory in the Era of B-Factories and CESR*, Stanford, CA, August 15-16, 1994

$\sqrt{s}$ GeV	Particle	Cross Section (nb)	Pairs Produced ($\times 10^8$)
3.77	$D^0\bar{D}^0$	5.8 ± 0.8	1.0
3.77	D^+D^-	4.2 ± 0.7	0.8
4.03	$D_s\bar{D}_s$	0.7 ± 0.2	0.24
4.14	$D_s\bar{D}_s^*$	0.9 ± 0.2	0.32

Table 1. Charm production cross sections and rates.

The exclusive nature of charm production at a τcF automatically supplies the production kinematics and low combinatoric backgrounds that are essential to background rejection. The charm production cross section in this energy region is large and well measured, as can be seen in Table 1 from Ref. [3]. Although the largest production rates occur at threshold, the proposed B-Factories and a high luminosity Z Factory could produce a comparable (but slightly smaller) number of charmed particles. The advantage of the threshold region at a τcF is that it provides the capability to control backgrounds and systematic errors. Since the beam energy can be tuned to lie just below or above production threshold, physics backgrounds can be directly measured, instead of estimated via Monte Carlo simulations. Because heavy flavors are pair produced at threshold, the observation of the decay of one particle, cleanly tags its partner. This yields a sample[3] of $10^6 - 10^7$ singly tagged D-mesons per year, a size which is crucial in order to obtain highly precise measurements of branching fractions and to search for rare processes.

The charm physics program at a τcF is strong and diverse. Charm hadrons possess a rich variety of weak decays: Cabibbo allowed, single Cabibbo suppressed, double Cabibbo suppressed, leptonic, semileptonic, and rare higher-order decays. The scale of the interactions is in the middle of the regime where perturbative and non-perturbative QCD effects are cleanly separable. Hence the charm system provides an excellent laboratory to test our understanding of QCD, the dynamics of heavy quark decay, and the structure of the hadronic weak current. The knowledge gained from a comprehensive study would supply the needed benchmarks for lattice QCD and result in a more reliable extrapolation to the B system. Fundamental parameters in the SM, such as the values of the Cabbibo-Kobayashi-Maskawa (CKM) mixing matrix elements involving charm-quark decay, would also be more precisely determined. The charm system also offers the opportunity to study CP violation in the up-quark sector and to search for new sources of CP violation. Loop induced processes are very sensitive to new particles which may participate in the loop and hence may provide a signature for physics beyond the SM. Rare charm interactions compliment searches in the down-quark sector because the couplings to new particles may be flavor dependent, either through mass dependent couplings or through mixing angles.

We now turn to a discussion of semileptonic, leptonic, hadronic, rare and forbidden decays of the charm quark, as well as $D^0 - \bar{D}^0$ mixing and CP violation in the charm sector. In each case we (i) review the motivation for studying these processes,

(ii) summarize the present status of theoretical calculations in the SM and beyond, and (iii) examine the experimental sensitivities available at a tau-charm factory. Further details can be found in Refs. [4,5].

2. Semileptonic Decays of Charmed Hadrons

Semileptonic decays occupy a fundamental place in the experimental study of charm decays and in attempts to understand the underlying dynamics associated with charmed hadrons. They also play a critical role in determining the elements of the CKM mixing matrix. However, the extraction of the values for the CKM elements requires knowledge of the form factors which parameterize the matrix elements of the hadronic weak current. Theoretical calculation of these form factors is a thorny problem, particularly in the case of charm decays as they occur at an energy scale which lies between the regimes where chiral perturbation theory and heavy quark mass expansions (which are used to describe K and B decays, respectively) are absolutely valid. With the exception of lattice calculations, the form factors cannot be calculated from first principles, and thus model dependent estimates, usually combined with approximate symmetry properties, must be employed. It is therefore crucial to measure the shape of the form factors in order to test the theoretical models. This would enhance our understanding of QCD, and enable scaling of the predictions to the B sector with better accuracy, as well as provide an improved determination of the CKM matrix elements in the charm sector.

Before turning to a discussion of the form factors, we first note that the CKM elements governing semileptonic charm decay, V_{cd} and V_{cs}, are surprisingly poorly determined at present. The best determination of V_{cd} is from charm production in neutrino scattering off valence d-quarks, yielding the value[6] $|V_{cd}| = 0.204 \pm 0.017$. Extracting V_{cs} from this method is plagued by uncertainties from the estimates of the strange quark parton density and hence the semileptonic decay $D^+ \to \bar{K} e^+ \nu$ is used. Comparison of the data with theory and using conservative assumptions in calculating the form factors yields[6] $|V_{cs}| = 1.01 \pm 0.18$. The imposition of CKM unitarity for a three generation SM constrains[6] the values of these elements further to $|V_{cd}| = 0.221 \pm 0.003$ and $|V_{cs}| = 0.9745 \pm 0.0007$. We see that these CKM elements are very well known if one *assumes* unitarity, but that the direct experimental measurements are at the $10 - 20\%$ level. There are many theories beyond the SM which preclude a three generation unitary CKM matrix and they should be tested with a precision in the charm sector that is equivalent to that of planned experiments in the B system. For example, the comparison of the exclusive semileptonic decays $D \to \pi \mu \nu$ and $D \to K \mu \nu$, where theoretical uncertainties mostly cancel in taking the ratio, would allow a determination of $|V_{cd}|/|V_{cs}|$ to $\sim 1\%$, which is comparable to the present level of precision on the Cabibbo angle θ_c.

Semileptonic rates are dominated by modes containing only one hadron in the final state. These are K or K^* for Cabibbo allowed decay, π or ρ for Cabibbo suppressed D decay, and η, η', ϕ for Cabibbo suppressed D_s decay. For the decay into a pseudoscalar

meson, $D \to P\ell\nu$, the hadronic matrix element can be written as

$$\langle P(k)|\bar{q}\gamma_\mu c|D(p)\rangle = f_+(q^2)(p+k)_\mu + f_-(q^2)(p-k)_\mu\,, \tag{1}$$

where $q^2 = (p-k)^2$ is the momentum transfer and $\bar{q} = \bar{s}, \bar{d}$ for $P = K, \pi$, respectively. If the lepton mass is neglected, only f_+ contributes to the q^2 distribution with

$$\frac{d\Gamma}{dq^2} = \frac{G_F^2|V_{cs(d)}|^2 k^3}{24\pi^3}|f_+(q^2)|^2\,. \tag{2}$$

We note that an accurate comparison of the rate for $D \to Ke\nu$ to that for $D \to K\mu\nu$ would determine $f_-(q^2)$ and provide the best direct measurement of V_{cs}.

Theoretical uncertainties are introduced by assuming a particular q^2 dependence of the form factor. It is usually parameterized using vector meson dominance with

$$f_+(q^2) = \frac{f_+(0)}{1 - q^2/m^{*2}}\,, \tag{3}$$

where m^* is the pole mass of the appropriate channel. This method allows one to fit and determine the pole mass. In heavy quark effective theory (HQET), all decay modes are described in terms of a single form factor assuming an exponential q^2 dependence, $f_+(q^2) = f_+(0)\exp(\alpha q^2)$. This yields values of $f_+(0)$ which are approximately 5% smaller than those obtained in the single pole ansatz. However, HQET is less advantageous in D decays as the symmetry breaking corrections as expected to be large. Various theoretical predictions[7] (from quark model calculations, QCD sum rules, and lattice QCD) for the form factor in $D \to K\ell\nu$, as well as the average experimental result,[6] including a recent determination by CLEO[8] from a measurement of the q^2 distribution, is summarized in Table 2. In the case of the monopole distribution, the pole mass is then measured to be $m^* = (2.00 \pm 0.12 \pm 0.18)\,\mathrm{GeV}$, which is consistent with the D_s^* mass. For HQET, the fit value of α is $\alpha = (0.29 \pm 0.04 \pm 0.06)\,\mathrm{GeV}^{-2}$, which should be compared with the predicted value[7] of $\alpha = 0.21\,\mathrm{GeV}^{-2}$.

The various quark model predictions for the q^2 dependence are in rough agreement with each other as they all incorporate a recoil energy dependence that reflects a fall-off with a typical hadronic scale of $\sim 1\,\mathrm{GeV}$. Large disagreements in the predictions will only occur either at low energies, if there are poles close to the physical region, or at recoil energies greater than 1 GeV. Therefore charm meson semileptonic decays do not fully probe the different aspects of the models given the limited kinematic range. Very precise measurements will then be needed in order to discriminate amongst the models.

For semileptonic decay to a vector meson V, the hadronic matrix element can be parameterized in terms of four form factors,

$$\langle V(k)|\bar{q}\gamma_\mu c|D(p)\rangle \;=\; \frac{2V(q^2)}{m_D + m_V}\epsilon_{\mu\nu\alpha\beta}\epsilon^{*\nu}p^\alpha k^\beta\,, \tag{4}$$

Reference	$f_+(0)$	$V(0)$	$A_1(0)$	$A_2(0)$
Exp. Average	$0.75 \pm 0.02 \pm 0.02$	1.1 ± 0.2	0.56 ± 0.04	0.40 ± 0.08
Theory				
ISGW	0.82	1.1	0.8	0.8
BSW	0.76	1.3	0.88	1.2
AW	0.7	1.5	0.8	0.6
BKS	$0.90 \pm 0.08 \pm 0.21$	$1.4 \pm 0.5 \pm 0.5$	$0.8 \pm 0.1 \pm 0.3$	$0.6 \pm 0.1 \pm 0.2$
LMMS	0.63 ± 0.08	0.9 ± 0.1	0.53 ± 0.03	0.2 ± 0.2
BBD	0.60	1.1	0.5	0.6

Table 2. Measured and predicted form factors in $D \to K\ell\nu$ and $D \to K^*\ell\nu$.

Reference	$\Gamma(D \to K^*\ell\nu)/\Gamma(D \to K\ell\nu)$
Experiment	0.58 ± 0.06
ISGW	1.14
BSW	0.87
AW	1.34
BBD	0.6 ± 0.4

Table 3. Theoretical predictions and experimental average for the ratio $\Gamma(D \to K^*\ell\nu)/\Gamma(D \to K\ell\nu$.

$$\langle V(k)|\bar{q}\gamma_\mu\gamma_5 c|D(p)\rangle = i\left[(m_D+m_V)A_1(q^2)\epsilon^*_\mu - \frac{A_2(q^2)}{m_D+m_V}\epsilon^*\cdot p(p+k)_\mu + \frac{2m_V}{q^2}A_3(q^2)\epsilon^*\cdot p(p-k)_\mu\right],$$

where ϵ represents the polarization vector of V. The contribution from $A_3(q^2)$ vanishes in the limit of massless leptons. Here, branching fraction measurements alone do not allow the determination of the form factors, and angular distributions must also be measured in order to extract all three. A summary of existing form factor measurements[6] and various theoretical predictions[7] is displayed in Table 2 for comparison purposes. We see that most calculations agree, within errors, with the experimental determination of $V(0)$, but fail to predict $A_1(0)$ and $A_2(0)$.

Theoretical predictions[7] for the ratio of vector to pseudoscalar decay modes are compared to the experimental averaged result[6] in Table 3. We see that the QCD sum rule approach (BBD) obtains the best agreement with experiment, but also has large errors. The agreement with the $f_+(0)$ measurements seen in Table 2 points to the K^* mode as the problem, which is also in accord with our conclusions on the axial vector form factors in Table 2. Since we seem to lack a clear theoretical understanding of these decays, accurate experimental information in several modes is vital.

There are two recent experimental measurements of the vector and axial-vector

Reference	$V(0)/A_1(0)$	$A_2(0)/A_1(0)$
Exp. Average	2.0 ± 0.7	1.8 ± 0.5
SI	1.85	1.21
BKS	$2.00 \pm 0.19 \pm 0.23$	$0.78 \pm 0.08 \pm 0.15$
LMMS	1.65 ± 0.2	0.33 ± 0.36

Table 4. Measured and calculated form factors in $D_s \to \phi\ell\nu$.

form factors in D_s decays. They constitute a further opportunity to examine the discrepancies between theory and experiment which appear to exist in D decay. Table 4 summarizes the measured[6] and predicted[7] form factors in the decay $D_s \to \phi\ell\nu$. We see that theory fails to provide the correct value for the ratio $A_2(0)/A_1(0)$, just as in the K^* mode. It would be of interest to investigate the process $D_s \to (\eta + \eta')\ell\nu$ to see if the disagreement between theory and experiment persists only in the vector mode as in the case of D decays.

Charmed baryon semileptonic decays provide yet another opportunity to test theoretical calculations. For example, a measurement of $\Lambda_c^+ \to \Lambda\ell\nu$, which is expected to dominate the Λ_c semileptonic decays, would yield information on heavy quark predictions that relate these decays to $D \to X_s\ell\nu$. Measurement of the Λ_c and Ξ_c branching factions would supply essential input to the analysis of the charm content in B decays.

A study of inclusive semileptonic decays would provide an additional test of HQET, as well as allowing for the extraction of a value for the charm quark mass. The results of a recent HQET analysis[9] from present data on charm semileptonic decays yield $m_c = 1.57 \pm 0.03 \pm 0.05\,\mathrm{GeV}$, where the errors represent the experimental and theoretical uncertainties, respectively. Another important question to be addressed is whether the sum of the exclusive rates saturate the inclusive rate.

With adequate statistics, the exclusive semileptonic rates as well as the q^2 dependences and relative normalization of the form factors can be measured at a τcF. The ability to make efficient measurements over the full kinematic range is essential. The expected number[3] of detected exclusive modes per year at a τcF lies in the range $10^4 - 10^5$ for the various channels in D^0, D^+ decay and $10^3 - 10^4$ for D_s. Figure 1 from Ref. [10] displays the use of tagging, kinematics, and calorimetry to isolate Cabbibo allowed and suppressed decays by the method of reconstructing the missing mass. This analysis shows that the events are expected to be essentially background free. A τcF could provide an exhaustive and accurate data base, with which the various theoretical models could be compared, and allows for the reliable determination of the CKM elements governing charm-quark decay.

Meson	$\mu^+\nu_\mu$	$\tau^+\nu_\tau$
D^+	3.52×10^{-4}	9.34×10^{-4}
D_s^+	4.21×10^{-3}	4.11×10^{-2}

Table 5. SM branching fractions for the leptonic decay modes, assuming $f_D = 200\,\mathrm{MeV}$ and $f_{D_s} = 230\,\mathrm{MeV}$.

3. Leptonic Decays of Charmed Mesons

The SM transition rate for the purely leptonic decay of a pseudoscalar charm meson is

$$\Gamma(D^+_{(q)} \to \ell^+\nu_\ell) = \frac{G_F^2}{8\pi} f_{D_{(q)}} |V_{cq}|^2 m_{D_{(q)}} m_\ell^2 \left(1 - \frac{m_\ell^2}{m^2_{D_{(q)}}}\right)^2 , \tag{5}$$

with $q = d, s$ and $f_{D(q)}$ is the weak decay constant defined as usual by

$$\langle 0|\bar{q}\gamma_\mu\gamma_5 c|D_{(q)}(\mathbf{p})\rangle = i f_{D_{(q)}} p_\mu \,, \tag{6}$$

where $f_\pi = 131\,\mathrm{MeV}$ in this normalization. The resulting branching fractions are small due to the helicity suppression and are listed in Table 5 using the central values of the CKM parameters given in Ref. [6] and assuming $f_D = 200\,\mathrm{MeV}$ and $f_{D_s} = 230\,\mathrm{MeV}$.

Assuming that the CKM matrix elements are well-known, the leptonic decays can provide important information on the value of the pseudoscalar decay constants. Precise measurements of these constants are essential for the study of $D^0 - \bar{D}^0$ mixing, CP violation in the charm sector, and non-leptonic decays. They would also test the accuracy of QCD calculational techniques and provide a means for more precise predictions when extrapolating to the B sector. The existing upper limit for f_D is $f_D < 290\,\mathrm{MeV}$, and is derived from the 90% C.L. bound[11] $B(D^+ \to \mu^+\nu_\mu) < 7.2 \times 10^{-4}$. CLEO has recently observed[12] the process $D_s^{*+} \to D_s^+\gamma \to \mu\nu\gamma$ by examining the mass difference $\delta M \equiv M_{\mu\nu\gamma} - M_{\mu\nu}$ and have obtained

$$\frac{\Gamma(D_s^+ \to \mu^+\nu)}{\Gamma(D_s^+ \to \phi\pi^+)} = 0.235 \pm 0.045 \pm 0.063 \,. \tag{7}$$

Using $\Gamma(D_s^+ \to \phi\pi^+) = 3.7 \pm 1.2\%$ they find $f_{D_s} = 337 \pm 34 \pm 45 \pm 54\,\mathrm{MeV}$ where the last error reflects the uncertainty in the $\phi\pi^+$ branching fraction. An emulsion experiment has measured[13] $f_{D_s} = 232 \pm 45 \pm 52\,\mathrm{MeV}$. The BES Collaboration has also recently reported[14] the observation of three candidate events in $e^+e^- \to D_s^+ D_s^-$ with the subsequent decay $D_s \to \mu\nu$ yielding $f_{D_s} = 434^{+153}_{-133}\ {}^{+35}_{-33}\,\mathrm{MeV}$. The errors are expected to improve once more statistics are obtained.

A variety of theoretical techniques have been employed to estimate the value of f_D and f_{D_s}. Lattice QCD studies[15] calculate these quantities in the quenched approximation through a procedure that interpolates between the Wilson fermion scheme and the static approximation. The non-relativistic quark model is used to relate the decay

Decay Constant	Lattice	Quark Model	Sum Rule
f_D	$208(9) \pm 35 \pm 12$	207 ± 60	170 – 235
f_{D_s}	$230(7) \pm 30 \pm 18$	259 ± 74	204 – 270
f_{D_s}/f_D	$1.10(2) \pm 0.02 \pm 0.02 \pm 0.03$	1.25	1.21 ± 0.06

Table 6. Theoretical estimates of the weak decay constants in units of MeV, (taking $m_c = 1.3\,\mathrm{GeV}$ in the sum rule approach).

constant to the meson wave function at the origin, $f_M = \sqrt{12/M_M}\,|\psi(0)|$, which is then inferred from isospin mass splitting of heavy mesons.[16] Another approach uses QCD sum rules.[17] For each of these calculational methods, the resulting ranges for the values of the pseudoscalar decay constants are presented in Table 6. Given the large errors, the results of these three approaches are roughly consistent. The theoretical uncertainties associated with the ratio f_{D_s}/f_D are much smaller, as this ratio should deviate from unity only in the presence of broken SU(3) flavor symmetry. The magnitude of such flavor violating effects can be determined by the measurement of $B(D_s^+ \to \mu^+\nu_\mu)/B(D^+ \to \mu^+\nu_\mu)$. Obtaining precise values for these decay constants, both theoretically and experimentally, would provide valuable input for a wide range of phenomenological applications.

Non-SM contributions may affect the purely leptonic decays. Signatures for new physics include the measurement of non-SM values for the absolute branching ratios, or the observation of a deviation from the SM prediction

$$\frac{B(D_{(s)}^+ \to \mu^+\nu_\mu)}{B(D_{(s)}^+ \to \tau^+\nu_\tau)} = \frac{m_\mu^2\left(1 - m_\mu^2/m_{D_{(s)}}^2\right)^2}{m_\tau^2\left(1 - m_\tau^2/m_{D_{(s)}}^2\right)^2}\,. \tag{8}$$

This ratio is sensitive to violations of $\mu - \tau$ universality.

As an example, we consider the case where the SM Higgs sector is enlarged by an additional Higgs doublet. These models generate important contributions[18] to the decay $B \to \tau\nu_\tau$ and it is instructive to examine their effects in the charm sector. Two such models, which naturally avoid tree-level flavor changing neutral currents, are Model I, where one doublet (ϕ_2) generates masses for all fermions and the second (ϕ_1) decouples from the fermion sector, and Model II, where ϕ_2 gives mass to the up-type quarks, while the down-type quarks and charged leptons receive their mass from ϕ_1. Each doublet receives a vacuum expectation value v_i, subject to the constraint that $v_1^2 + v_2^2 = v_{\rm SM}^2$. The charged Higgs boson present in these models will mediate the leptonic decay through an effective four-Fermi interaction, similar to that of the SM W-boson. The $H^\pm$ interactions with the fermion sector are governed by the Lagrangian

$$\begin{aligned}\mathcal{L} \;=\; & \frac{g}{2\sqrt{2}M_W} H^\pm [V_{ij} m_{u_i} A_u \bar{u}_i (1-\gamma_5) d_j + V_{ij} m_{d_j} A_d \bar{u}_i (1+\gamma_5) d_j \\ & m_\ell A_\ell \bar{\nu}_\ell (1+\gamma_5)\ell] + h.c.\,,\end{aligned} \tag{9}$$

with $A_u = \cot\beta$ in both models and $A_d = A_\ell = -\cot\beta(\tan\beta)$ in Model I(II), where $\tan\beta \equiv v_2/v_1$. In Models I and II, we obtain the result

$$B(D^+ \to \ell^+\nu_\ell) = B_{\rm SM}\left(1 + \frac{m_D^2}{m_{H^\pm}^2}\right)^2 , \tag{10}$$

where in Model II the D_s^+ decay receives an additional modification

$$B(D_s^+ \to \ell^+\nu_\ell) = B_{\rm SM}\left[1 + \frac{m_{D_s}^2}{m_{H^\pm}^2}\left(1 - \tan^2\beta\frac{m_s}{m_c}\right)\right]^2 . \tag{11}$$

In this case, we see that the effect of the $H^\pm$ exchange is independent of the leptonic final state and the above prediction for the ratio in Eq. (8) is unchanged. This is because the $H^\pm$ contribution is proportional to the charged lepton mass, which is then a common factor with the SM helicity suppressed term. However, the absolute branching fractions can be modified; this effect is negligible in the decay $D^+ \to \ell^+\nu_\ell$, but could be of order a few percent in D_s^+ decay if $\tan\beta$ is very large.

The detection of $D^+, D_s^+ \to \mu^+\nu$ decays is straightforward with single tagged event samples at a τcF allowing the measurement of the weak decay constants at the 1% level.[19] The $\tau^+\nu$ modes can also be observed via the subsequent decays $\tau \to \pi\nu, \ell\nu\nu$ by relying on tagging, hermiticity, and background measurements. The tagged event samples are used to provide a constrained fit for the neutrino mass as well as to suppress backgrounds. Figure 2 from Ref. [19] shows that the missing mass spectrum cleanly separates the signal from background in all cases.

4. Nonleptonic Decays of Charm Hadrons

Nonleptonic charm decays provide another opportunity to test our theoretical understanding of heavy flavor decays. They occur in a regime where non-perturbative effects are more (less) important than in B (K) decays. The thorough investigation of the rich variety of decay processes available would unravel these QCD effects and would build a foundation for a more reliable extrapolation to the underlying dynamics in the B system. Several types of processes mediate nonleptonic charm decays, *e.g.*, external spectator, color suppressed or internal spectator, weak annihilation, exchange, penguin, and mixing. Disentangling the underlying quark processes and determining their relative strengths is difficult and will require an increase of $2-3$ orders of magnitude over current statistics, but will generate a detailed understanding of strong interaction effects.

The absolute branching fractions of hadronic charm decays need to be measured with better precision. The present sensitivity of measurements of D^0 and D^+ decay is at the $10-20\%$ level, while the situation for D_s is even more uncertain as the absolute scale of its branching fractions is unknown. Most D_s decays are measured relative to the $\phi\pi^+$ mode, which is determined from the ratio $\Gamma(D_s^+ \to \phi e^+\nu)/\Gamma(D_s^+ \to \phi\pi^+)$ combined with estimates of the D_s^+ cross section, theoretical predictions relating D^+

and D_s^+ decays, and fragmentation assumptions. A direct determination of the $\phi\pi^+$ branching fraction could thus shift the values of the remaining branching fractions. Very few of the rates for charm baryon decay (particularly for Ξ_c and Ω_c) have been measured. Accurate data on these modes would provide invaluable assistance in the determination of the charm content in B decays, CP violating asymmetries, and in fragmentation studies.

The τcF is well suited[3] for these measurements. The increase in statistics and the efficient single and double tagging techniques allows the determination of the absolute branching fractions for D^0 and D^+ at the 1% level, limited only by systematics. Approximately 5×10^5 single D_s tags can be reconstructed in one year at $10^{33}\,\mathrm{cm}^{-2}\,\mathrm{sec}^{-1}$ using the $\phi\pi^+\,, S^*\pi^+\,, \bar{K}^0K^+$ and $\bar{K}^{*0}K^+$ decay modes, while the number of double tags from pairing these channels is $4950 \times B(\phi\pi^+)$. This yields a $\sim 3\%$ sensitivity to the absolute scale of D_s decays. Similar absolute measurements of charm baryon decays could also be performed.

D mesons are sufficiently heavy for many body final states to play a prominent role in their nonleptonic modes, however, D^0 and D^+ decays presently appear to be dominated by two body modes. In this case, most of the theoretical work is based on factorization[20] or QCD sum rule[21] approaches. The latter technique yields approximately model independent predictions for the amplitudes of four decay types $D\,, D_s \to PP, PV$, where $P(V)$ is a pseudoscalar (vector) meson built of light quarks, but the numerical results depend on the assumption of $SU(3)$ flavor symmetry. The former method is based on PP, VP, VV, and AP final states (where A represents an axial-vector meson) and assumes, (i) an amplitude which is expressed as the product of two current matrix elements, *i.e.*,

$$\langle M_1 M_2 | J^\mu J_\mu | D \rangle \simeq \langle M_1 | J^\mu | 0 \rangle \cdot \langle M_2 | J_\mu | D \rangle \,, \tag{12}$$

(ii) two fit parameters, a_1 and a_2, which occur in the nonleptonic weak Hamiltonian

$$\mathcal{H}^{eff} = -\frac{G_F}{\sqrt{2}} : [a_1(\bar{u}d')(\bar{s}'c) + a_2(\bar{s}'d')(\bar{u}c)] : , \tag{13}$$

where the colons denote Wick ordering and d', s' are Cabbibo rotated, (iii) model dependencies for the hadronic wavefunctions, and (iv) that the contributions from penguin amplitudes and final state interactions are negligible. This model currently provides a reasonable description for D^0 and D^+ decay modes, but may not hold up once more accurate data is obtained. The systematic study and comparison of D and B decays will help clarify some of the unresolved issues and inherent model dependencies associated with factorization.

The situation with D_s decays is not so well described. The anticipated strength of the weak annihilation process has yet to be confirmed and it is possible that the pattern of D_s decays may not mimic those of D^0 and D^+. It has been suggested[21] that the D_s may have an enhanced non-resonant width into multi-particle final states. In this

case, the constraints of production at threshold help to reconstruct these complicated many body modes. An reconstruction example from Ref. [3] at $\sqrt{s} = 4.028\,\mathrm{GeV}$ for $D_s \to \eta\pi^+\pi^+\pi^-$ with the subsequent decays $\eta \to \pi^+\pi^-\pi^0$ and $\pi^0 \to \gamma\gamma$ is depicted in Fig. 3.

Doubly suppressed Cabibbo decays, having branching fractions of order $\tan^4\theta_c$ relative to Cabbibo allowed decays, also test our understanding of the hadronic weak current. These modes are best measured by tagging in D^+ decays, since there is no confusion with the possible mixing component which may be present in D^0 modes. A handful of events in $D^+ \to K^+K^+K^-, \phi K^+$ and $D^0 \to K^+\pi^-$ have been observed.[6] It is expected[3] that a few hundred such events can be reconstructed at the τcF and that a signal sensitivity at the $\sim 10\%$ level can be achieved.

5. Rare and Forbidden Decays of Charm Mesons

Flavor changing neutral current (FCNC) decays only occur at the loop level in the SM. Due to the effectiveness of the GIM mechanism and the small masses of the quarks which participate inside the loops, short distance SM contributions to rare charm decays are very small. Most reactions are thus dominated by long distance effects which are difficult to reliably calculate. However, a recent investigation[4] of such effects indicates that there is a window for the clean observation of new physics in some interactions. In fact, it is precisely because the SM FCNC rates are so small, that charm provides an important opportunity to discover new effects, and offers a detailed test of the SM in the up-quark sector.

FCNC decays of the D meson include the processes $D^0 \to \ell^+\ell^-, \gamma\gamma$, and $D \to X + \ell^+\ell^-, X + \nu\bar{\nu}, X + \gamma$, with $\ell = e, \mu$. They proceed via electromagnetic or weak penguin diagrams as well as receiving contributions from box diagrams in some cases. The calculation of the SM short distance rates for these processes is straightforward and the transition amplitudes and standard loop integrals, which are categorized in Ref. [22] for rare K decays, are easily converted to the D system. The loop integrals relevant for $D^0 \to \gamma\gamma$ may be found in Ref. [23]. Employing the GIM mechanism results in a general expression for the loop integrals which can be written as

$$A = V_{cs}V_{us}^*[F(x_s) - F(x_d)] + V_{cb}V_{ub}^*[F(x_b) - F(x_d)]\,, \tag{14}$$

with $x_i \equiv m_i^2/M_W^2$ and $F(x_d)$ usually being neglected (except in the 2γ case). The s- and b-quark contributions are roughly equal as the larger CKM factors compensate for the small strange quark mass. The values of the resulting inclusive short distance branching fractions, before QCD corrections are applied, are shown in Table 7, along with the current experimental bounds.[6,24] The corresponding exclusive rates are typically an order of magnitude less than the inclusive case. We note that the transition $D^0 \to \ell^+\ell^-$, is helicity suppressed and hence has the smallest branching fraction. The range given for this branching fraction, $(1 - 20) \times 10^{-19}$, indicates the effect of varying the parameters in the ranges $f_D = 0.15 - 0.25\,\mathrm{GeV}$ and $m_s = 0.15 - 0.40\,\mathrm{GeV}$.

Decay Mode	Experimental Limit	$B_{S.D.}$	$B_{L.D.}$
$D^0 \to \mu^+\mu^-$	$< 1.1 \times 10^{-5}$	$(1-20) \times 10^{-19}$	$< 3 \times 10^{-15}$
$D^0 \to e^+e^-$	$< 1.3 \times 10^{-4}$		
$D^0 \to \mu^\pm e^\mp$	$< 1.0 \times 10^{-4}$	0	0
$D^0 \to \gamma\gamma$	—	10^{-16}	$< 3 \times 10^{-9}$
$D \to X_u + \gamma$		1.4×10^{-17}	
$D^0 \to \rho^0\gamma$	$< 1.4 \times 10^{-4}$		$< 2 \times 10^{-5}$
$D^0 \to \phi^0\gamma$	$< 2.0 \times 10^{-4}$		$< 10^{-4}$
$D^+ \to \rho^+\gamma$	—		$< 2 \times 10^{-4}$
$D^+ \to \bar{K}^{*+}\gamma$	—		3×10^{-7}
$D^0 \to \bar{K}^{*0}\gamma$	—		1.6×10^{-4}
$D \to X_u + \ell^+\ell^-$		4×10^{-9}	
$D^0 \to \pi^0\mu\mu$	$< 1.7 \times 10^{-4}$		
$D^0 \to \bar{K}^0 ee/\mu\mu$	$< 17.0/2.5 \times 10^{-4}$		$< 2 \times 10^{-15}$
$D^0 \to \rho^0 ee/\mu\mu$	$< 2.4/4.5 \times 10^{-4}$		
$D^+ \to \pi^+ ee/\mu\mu$	$< 250/4.6 \times 10^{-5}$	few$\times 10^{-10}$	$< 10^{-8}$
$D^+ \to K^+ ee/\mu\mu$	$< 480/8.5 \times 10^{-5}$		$< 10^{-15}$
$D^+ \to \rho^+\mu\mu$	$< 5.8 \times 10^{-4}$		
$D^0 \to X_u + \nu\bar{\nu}$		2.0×10^{-15}	
$D^0 \to \pi^0\nu\bar{\nu}$	—	4.9×10^{-16}	$< 6 \times 10^{-16}$
$D^0 \to \bar{K}^0\nu\bar{\nu}$	—		$< 10^{-12}$
$D^+ \to X_u + \nu\bar{\nu}$	—	4.5×10^{-15}	
$D^+ \to \pi^+\nu\bar{\nu}$	—	3.9×10^{-16}	$< 8 \times 10^{-16}$
$D^+ \to K^+\nu\bar{\nu}$	—		$< 10^{-14}$

Table 7. Standard Model predictions for the branching fractions due to short and long distance contributions for various rare D meson decays. Also shown are the current experimental limits.

The calculation of the long distance branching fractions are plagued with the usual hadronic uncertainties and the estimates listed in the table convey an upper limit on the size of these effects rather than an actual value. These estimates have been computed by considering various intermediate particle states (*e.g.*, $\pi, K, \bar{K}, \eta, \eta', \pi\pi,$ or $K\bar{K}$) and inserting the known rates for the decay of the intermediate particles into the final state of interest. In all cases we see that the long distance contributions overwhelm those from SM short distance physics

The radiative decays, $D \to X + \gamma$, merit further discussion. One of the goals of a high luminosity B physics program is to extract the ratio of CKM elements $|V_{td}|/|V_{ts}|$ from a measurement of $B(B \to \rho/\omega + \gamma)/B(B \to K^*\gamma)$. CLEO has placed[25] a bound on this ratio of branching fractions of < 0.34, while observing the decay $B \to K^*\gamma$ with a branching fraction of $(4.5 \pm 1.5 \pm 0.9) \times 10^{-5}$. This yields a very loose constraint on the above ratio of CKM elements. This method of determining the ratio of CKM elements depends critically on the assumption that these exclusive decay modes are dominated by short distance penguin transitions. If this assumption is false, and the long distance contributions to these decays were found to be large, this technique would be invalidated. Unfortunately, the theoretical uncertainties associated with computing the long distance contributions are sizeable.[26] Where separation of the two types of contributions is somewhat difficult in the B sector, radiative charm decays provide an excellent testing ground. In this case it should be possible to separate out the inclusive penguin transitions $c \to u\gamma$, and determine the rate of the long distance reactions which are expected to dominate. For example, the penguin transitions do not contribute to $D^0 \to \bar{K}^{*0}\gamma$ and it would be a direct measurement of the non-perturbative effects. Before QCD corrections are applied, the short distance inclusive rate is very small, $B(c \to u\gamma) = 1.4 \times 10^{-17}$; however, the QCD corrections *greatly* enhance this rate.[27] These corrections are calculated via an operator product expansion, where the effective Hamiltonian is evolved at leading logarithmic order from the electroweak scale to down to the charm quark scale by the Renormalization Group Equations. This procedure mirrors that used for $b \to s\gamma$, and results in $B(c \to u\gamma) = (1.1 - 2.3) \times 10^{-5}$, where the lower(upper) value corresponds to taking the scale of the decay to be $2m_c(m_c)$. (We note that these radiative branching fractions have been scaled to semileptonic charm decay in order to reduce the CKM and m_c uncertainties.) In this case, the rate is given almost entirely by operator mixing! The penguin contributions to the exclusive channels would then be typically of order 10^{-6}, which is still smaller than the long distance estimates in Table 7. Observation of

$$\frac{B(D^0 \to \rho^0\gamma)}{B(D^0 \to \bar{K}^{*0}\gamma)} \neq \tan^2\theta_c \tag{15}$$

at the few percent level would be a test of the perturbative QCD corrections, or it could be a signal for new physics. We note that the predicted values of the branching fractions for radiative charm decays are well within reach of the τcF.

Lepton flavor violating decays, *e.g.*, $D^0 \to \mu^\pm e^\mp$ and $D \to X + \mu^\pm e^\mp$, are strictly

forbidden in the SM with massless neutrinos. In a model with massive non-degenerate neutrinos and non-vanishing neutrino mixings, such as in four generation models, $D^0 \to \mu^\pm e^\mp$ would be mediated by box diagrams with the massive neutrinos being exchanged internally. LEP data restricts[28] heavy neutrino mixing with e and μ to be $|U_{Ne}U^*_{N\mu}|^2 < 7\times10^{-6}$ for a neutrino with mass $m_N > 45\,\mathrm{GeV}$. Consistency with this bound constrains the branching fraction to be $B(D^0 \to \mu^\pm e^\mp) < 6 \times 10^{-22}$. This same results also holds for a heavy singlet neutrino which is not accompanied by a charged lepton. The observation of this decay at a larger rate than the above bound would be a clear signal for the existence of a different class of models with new physics.

Examining Table 7, we see that there is a large window of opportunity to discover the existence of new physics in rare charm decays. Although the SM short distance contributions are completely dominated by the long distance effects, there are some modes where the size of the two contributions are not that far apart. The observation of any of these modes at a larger rate than what is predicted from long distance interactions would provide a clear signal for new physics. To demonstrate the magnitude of enhancements that are possible in theories beyond the SM, we consider two examples (i) a heavy $Q = -1/3$ quark contributing to $D \to X + \ell^+\ell^-$ and (ii) leptoquark exchange mediating $D^0 \to \mu^\pm e^\mp$. In the first case, a heavy $Q = -1/3$ quark may be present, *e.g.*, as an iso-doublet fourth generation b' quark, or as a singlet quark in E_6 grand unified theories. The current bound[6] on the mass of such an object is $m_{b'} > 85\,\mathrm{GeV}$, assuming that it decays via charged current interactions. The heavy quark will then participate inside the penguin and box diagrams which mediate the decay and result in the branching fractions presented in Fig. 4. The branching fractions are displayed as functions of the overall CKM mixing factor for several values of the heavy quark mass, and we see that a sizeable enhancement is possible for large values of the mixing. A naive estimate in the four generation SM yields[6] the restrictions $|V_{cb'}| < 0.571$ and $|V_{ub'}| < 0.078$. In the second example of new physics contributions we consider leptoquark bosons. Leptoquarks are color triplet particles which couple to a lepton-quark pair and are naturally present in many theories beyond the SM which relate leptons and quarks at a more fundamental level. We parameterize their *a priori* couplings as $\lambda^2_{\ell q}/4\pi = F_{\ell q}\alpha$. Leptoquarks can mediate $D^0 \to \mu^\pm e^\mp$ by tree-level exchange, however their contributions are suppressed by angular momentum conservation. From the limit $B(D^0 \to \mu^\pm e^\mp) < 10^{-4}$, Davidson *et al.*[29] find

$$\sqrt{F_{eu}F_{\mu c}} < 4 \times 10^{-3} \frac{\alpha}{4\pi} \left[\frac{m_{LQ}}{100\,\mathrm{GeV}}\right]^2 , \tag{16}$$

where m_{LQ} represents the leptoquark mass.

Detector studies for the observation of loop-induced decays with leptonic final states $\ell^+\ell^-$ and $X + \ell^+\ell^-$ were performed in Ref. [30], where it was estimated that the level of background was $\leq 1 - 10$ events and that a τcF could search for these decays with branching fractions down to $(3 - 20) \times 10^{-8}$. This is an improvement of $3 - 5$ orders of magnitude over present limits and puts a τcF within striking range for some

of these modes. The radiative D decays will be able to be studied in detail at a τcF.

6. $D^0 - \bar{D}^0$ Mixing

Currently, the best limits[6] on $D^0 - \bar{D}^0$ mixing are from fixed target experiments, with $x_D \equiv \Delta m_D/\Gamma < 0.083$ (where $\Delta m_D = m_2 - m_1$ is the mass difference), yielding $\Delta m_D < 1.3 \times 10^{-13}\,\mathrm{GeV}$. The bound on the ratio of wrong-sign to right-sign final states is $r_D \equiv \Gamma(D^0 \to \ell^- X)/\Gamma(D^0 \to \ell^+ X) < 3.7 \times 10^{-3}$, where

$$r_D \approx \frac{1}{2}\left[\left(\frac{\Delta m_D}{\Gamma}\right)^2 + \left(\frac{\Delta\Gamma}{2\Gamma}\right)^2\right], \tag{17}$$

in the limit $\Delta m_D/\Gamma, \Delta\Gamma/\Gamma \ll 1$.

The short distance SM contributions to Δm_D proceed through a W box diagram with internal d, s, b-quarks. In this case the external momentum, which is of order m_c, is communicated to the light quarks in the loop and can not be neglected. The effective Hamiltonian is

$$\mathcal{H}_{eff}^{\Delta c=2} = \frac{G_F \alpha}{8\sqrt{2}\pi x_w}\left[|V_{cs}V_{us}^*|^2\left(I_1^s\mathcal{O} - m_c^2 I_2^s \mathcal{O}'\right) + |V_{cb}V_{ub}^*|^2\left(I_3^b\mathcal{O} - m_c^2 I_4^b\mathcal{O}'\right)\right], \tag{18}$$

where the I_j^q represent integrals[31] that are functions of m_q^2/M_W^2 and m_q^2/m_c^2, and $\mathcal{O} = [\bar{u}\gamma_\mu(1-\gamma_5)c]^2$ is the usual mixing operator while $\mathcal{O}' = [\bar{u}(1+\gamma_5)c]^2$ arises in the case of non-vanishing external momentum. The numerical value of the short distance contribution is $\Delta m_D \sim 5 \times 10^{-18}$ GeV (taking $f_D = 200\,\mathrm{MeV}$). The long distance contributions have been computed via two different techniques: (i) the intermediate particle dispersive approach (using current data on the intermediate states) yields[4,32] $\Delta m_D \sim 10^{-4}\Gamma \simeq 10^{-16}\,\mathrm{GeV}$, and (ii) heavy quark effective theory which results[33] in $\Delta m_D \sim (1-2) \times 10^{-5}\Gamma \simeq 10^{-17}\,\mathrm{GeV}$. Clearly, the SM predictions lie far below the present experimental sensitivity!

One reason the SM expectations for $D^0 - \bar{D}^0$ mixing are so small is that there are no heavy particles participating in the box diagram to enhance the rate. Hence the first extension to the SM that we consider is the addition[34] of a heavy $Q = -1/3$ quark. We can now neglect the external momentum and Δm_D is given by the usual expression,[22]

$$\Delta m_D = \frac{G_F^2 M_W^2 m_D}{6\pi^2} f_D^2 B_D |V_{cb'}V_{ub'}^*|^2 F(m_{b'}^2/M_W^2)\,. \tag{19}$$

The value of Δm_D is displayed in this model in Fig. 5a as a function of the overall CKM mixing factor for various values of the heavy quark mass. We see that Δm_D approaches the experimental bound for large values of the mixing factor.

Another simple extension of the SM is to enlarge the Higgs sector by an additional doublet as discussed in the above leptonic decay section. First, we examine two-Higgs-doublet models which avoid tree-level FCNC by introducing a global symmetry. The expression for Δm_D in these models can be found in Ref. [35]. ¿From the Lagrangian in

Eq. (9) it is clear that Model I will only modify the SM result for Δm_D for very small values of $\tan\beta$, and this region is already excluded[25,35] from existing data on $b \to s\gamma$ and $B_d^0 - \overline{B}_d^0$ mixing. However, enhancements can occur in Model II for large values of $\tan\beta$, as demonstrated in Fig. 5b.

Next we consider the case of extended Higgs sectors without natural flavor conservation. In these models the above requirement of a global symmetry which restricts each fermion type to receive mass from only one doublet is replaced[36] by approximate flavor symmetries which act on the fermion sector. The Yukawa couplings can then possess a structure which reflects the observed fermion mass and mixing hierarchy. This allows the low-energy FCNC limits to be evaded as the flavor changing couplings to the light fermions are small. We employ the Cheng-Sher ansatz,[36] where the flavor changing couplings of the neutral Higgs are $\lambda_{h^0 f_i f_j} \approx (\sqrt{2}G_F)^{1/2}\sqrt{m_i m_j}\Delta_{ij}$, with the $m_{i(j)}$ being the relevant fermion masses and Δ_{ij} representing a combination of mixing angles. h^0 can now contribute to Δm_D through tree-level exchange as well as mediating $D^0 - \bar{D}^0$ mixing by h^0 and t-quark virtual exchange in a box diagram. These latter contributions only compete with those from the tree-level process for large values of Δ_{ij}. In Fig. 6a we show the constraints placed on the parameters of this model from the present experimental bound on Δm_D for both the tree-level and box diagram contributions.

The last contribution to $D^0 - \bar{D}^0$ mixing that we will discuss here is that of scalar leptoquark bosons. They participate in Δm_D via virtual exchange inside a box diagram,[29] together with a charged lepton or neutrino. Assuming that there is no leptoquark-GIM mechanism, and taking both exchanged leptons to be the same type, we obtain the restriction

$$\frac{F_{\ell c} F_{\ell u}}{m_{LQ}^2} < \frac{196\pi^2 \Delta m_D}{(4\pi\alpha f_D)^2 m_D}\,, \tag{20}$$

where $F_{\ell q}$ is defined in the previous section. The resulting bounds in the leptoquark coupling-mass plane are presented in Fig. 6b.

Signatures for $D^0 - \bar{D}^0$ mixing include like-sign dileptons from $D^0\bar{D}^0 \to \ell^\pm\ell^\pm X$ or dual hadronic decays such as $D^0\bar{D}^0 \to K^\pm\pi^\mp K^\pm\pi^\mp$. The hadronic signal can be cleanly separated from double Cabbibo suppressed decays at a τcF since quantum statistics yield different correlations. This is due to the fact that the double Cabbibo suppressed modes can only contribute to the same final states when the D^0 mesons are in a relative S-wave. The interference with the doubly suppressed modes can also be used[37] to separate mixing which originates in the mass difference Δm_D from that which arises in the decay $\Delta\Gamma_D$. An extensive study of the double Cabbibo decays will result as a product of the search for $D^0 - \bar{D}^0$ mixing. A thorough Monte Carlo simulation of $D^0 - \bar{D}^0$ mixing at a τcF detector has been performed in Ref. [38], where the available sensitivity for mixing was found to be at the 10^{-5} level.

7. CP Violation

CP violation in the $Q = 2/3$ quark sector is complimentary to that of the K and B systems, but has yet to be explored. The τcF factory could thus provide an important first opportunity to explore CP violation in this sector. In the SM, the CKM phase is responsible for generating CP violation, and the resulting rates are small. However, new sources of CP violating phases could greatly enhance the rates thus rendering CP violation in the charm system a sensitive probe for physics beyond the SM.

CP violation requires the interference of at least two amplitudes with non-vanishing relative phases. This can occur indirectly via $D^0 - \bar{D}^0$ mixing, or directly via asymmetries induced in the decay amplitude, or kinematically in final state distributions. The first case corresponds to the interference of a D^0 decaying to a final state f at time t, with a D^0, which mixes into a $\bar{D}^0$ and then decays to f at time t. This process is theoretically clean as the hadronic uncertainties cancel in the asymmetry. However, since Δm_D is extremely small in the SM the induced CP violation is negligible. If new physics were to enhance $D^0 - \bar{D}^0$ mixing, as seen to occur in the previous section for some models, then this mechanism could yield sizeable CP violating effects.

Direct CP violation in charm meson decays yields slightly more promising results. Here, only decay amplitudes with two separate weak phases and two different strong phases will contribute. This can be easily seen as follows. Let us assume that the decay amplitude to final state f has the form

$$A_f = A_1 e^{i\delta_1} + A_2 e^{i\delta_2} \,, \tag{21}$$

with $A_{1,2}$ being the two amplitudes after the strong phases $\delta_{1,2}$ have been factored out. For the CP conjugate amplitude, the weak phases are conjugated, but the strong phases are not. The CP asymmetry is then given by

$$\frac{|A_f|^2 - |\bar{A}_{\bar{f}}|^2}{|A_f|^2 + |\bar{A}_{\bar{f}}|^2} = \frac{2\mathcal{I}m\,(A_1^* A_2)\sin(\delta_1 - \delta_2)}{|A_1|^2 + |A_2|^2 + 2\mathcal{R}e\,(A_1^* A_2)\cos(\delta_1 - \delta_2)} \,, \tag{22}$$

which clearly vanishes if $A_{1,2}$ contain the same weak phase and if $\delta_1 = \delta_2$. Before estimating the typical size of this asymmetry in the SM, we first note that in contrast to B decays, the branching fractions for the relevant modes, *i.e.*, $\pi^+\pi^-, K^+K^-$, etc., are rather sizeable in the charm system, and for once, the large effects of final state interactions are welcomed! Of course, this makes numerical predictions difficult due to the hadronic uncertainties associated with final state interaction phases. All tree-level interactions in D decays contain the same weak phase, hence they must interfere with penguin mediated processes in order to obtain the requisite two independent weak phases. Since Cabibbo favored modes are not mediated via penguin type interactions, only Cabibbo suppressed decays exhibit direct CP violation. Although the relative size of the tree and penguin contributions has not yet been determined, an upper bound for the size of the CP asymmetry is estimated[32,37,39] to be $a_{CP} < 10^{-3}$. However, there

could be a large enhancement from the strong interactions (which could be provided by, *e.g.*, nearby resonances) and typical results in this case are $a_{CP} \sim$ few $\times 10^{-3}$.

It is possible to obtain two separate weak phases in tree-level amplitudes in D_s decays, *i.e.*, via interference between the spectator and annihilation diagrams. If the annihilation processes are not suppressed relative to the spectator case, then CP asymmetries of order 10^{-3} are feasible.

Kinematic CP violation signals could occur, for example, in the decays $D \to VV$, which are described by more than one amplitude. Here, it is possible to construct CP-odd triple product correlations between the two polarizations and one of the momenta, *e.g.*, $\langle k \cdot \epsilon_1 \times \epsilon_2 \rangle$. Since final state interactions can induce a non-zero value of the triple product correlation and hence mask CP violation, one must evaluate

$$N_f = \frac{N(k \cdot \epsilon_1 \times \epsilon_2 > 0) - N(k \cdot \epsilon_1 \times \epsilon_2 < 0)}{N_{total}}\,, \tag{23}$$

as well as the corresponding quantity for $N_{\bar{f}}$, which vanish if CP is conserved. If N_f and $N_{\bar{f}}$ are determined to be non-zero then there is a clear signal of CP violation. Similar correlations have also been discussed[40] for semileptonic decays.

An interesting example of the potential size of CP violating effects from new physics is that of left-right symmetric models.[41,42] In this case reasonably large values for CP asymmetries can be obtained for the Cabbibo allowed decay modes. This occurs due to the existence of an additional amplitude from the W_R exchange, which carries a different weak phase from that of the W_L mediated decay. The estimated values of the CP asymmetries in these models is of order 0.01. Compared to the vanishing asymmetry obtained in the SM, this would provide a sizeable and clear signature for new physics.

The experimental feasibility of discovering CP violation at a τcF has been examined in detail,[38,37] as in the case of $D^0 - \bar{D}^0$ mixing, where Monte Carlo results indicate that the backgrounds to the two-body hadronic decays are manageable. These authors find that a τcF should be able to probe direct CP violating asymmetries in D decay at the level of 10^{-3}, which just touches the range predicted within the SM.

8. Summary

In summary we see that the charm physics program at a Tau-Charm factory is diverse and robust. We have seen that (i) it is possible to greatly improve the precision over present data samples on the charm system. Most decay modes as well as the pseudoscalar decay constants and the CKM elements governing charm-quark decay can be measured at a level of order 1%. This would greatly enhance our understanding of the underlying QCD interactions which govern these processes. In some decay modes and other interactions the τcF could provide the first opportunity for observation. (ii) Loop-induced reactions could be probed at a substantially increased level of sensitivity allowing for a wide window of opportunity to discover new physics. (iii) CP violation could finally be explored in the up-quark sector, where the capabilities of a τcF in

one year of running at design luminosity just touches the range of SM predictions. Several years of running (or increased luminosity) could study CP violation at the SM level. This wide physics potential and the high precision which can be achieved would place measurements in the charm sector at an equal level with those in the down-quark systems.

The τcF has the potential to address fundamental questions of the SM in a complimentary fashion to the on-going extensive studies of the down-quark sector.

References

1. M. Perl, these proceedings.
2. W. Toki, these proceedings.
3. R. Schindler, in *Proceedings of the Tau-Charm Factory Workshop*, SLAC, Stanford, CA, June 1989, SLAC-Report-343.
4. For further details, see, G. Burdman, E. Golowich, J. Hewett, and S. Pakvasa, Phys. Rep. (in preparation).
5. See also, τcF physics reviews, A. Pich in *Proceedings of the Marbella Workshop on the Tau-Charm Factory*, Marbella, Spain, June 1993; P. Roudeau, *ibid.*; A. Le Yaouanc *et al.*, Orsay Report, LPTHE-92/49 (1992); E. Gonzalez-Romero, Nucl. Phys. **A558**, 579c (1993).
6. L. Montanet *et al.*, Particle Data Group, Phys. Rev. **D50**, 1173 (1994).
7. N. Isgur, D. Scora, B. Grinstein, and M.B. Wise, Phys. Rev. **D39**, 799 (1989); M. Wirbel, B. Stech, and M. Bauer, Z. Phys. **C29**, 627 (1985); T. Altomari and L. Wolfenstein, Phys. Rev. **D37**, 681 (1988); C. Bernard, A. El Khadra, and A. Soni, Phys. Rev. **D43**, 2140 (1992); V. Lubicz, G. Martinelli, M.S. McArthy, and C.T. Sachrajda, Phys. Lett. **B274**, 415 (1992); P. Ball, V.M. Braun, and H.G. Dosch, Phys. Rev. **D44**, 3567 (1991).
8. A. Bean *et al.*, CLEO Collaboration, Phys. Lett. **B317**, 647 (1993).
9. I.I. Bigi and N.G. Uraltsev, Z. Phys. **C62**, 623 (1994).
10. J. Izen, in *Proceedings of the Tau-Charm Factory Workshop*, SLAC, Stanford, CA, June 1989, SLAC-Report-343.
11. MARK III Collaboration, Phys. Rev. Lett. **60**, 1375 (1988).
12. H., Yamamoto, these proceedings; CLEO Collaboration, Cornell Report CLNS-93-1238 (1993).
13. A. Aoki *et al.*, Prog. Theor. Phys. **89**, 131 (1993).
14. T., Huang, these proceedings.
15. C.W. Bernard, J.N. Labrenz, and A. Soni, Phys. Rev. **D49**, 2536 (1994).
16. J. Amundson *et al.*, Phys. Rev. **D47**, 3059 (1993); J. Rosner, Phys. Rev. **D42**, 3732 (1990).
17. C.A. Dominguez and N. Paver, Phys. Lett. **B318**, 629 (1993).
18. W.-S. Hou, Phys. Rev. **D48**, 2342 (1993); P. Krawczyk and S. Pokorski, Phys. Rev. Lett. **60**, 182 (1988).

19. P.C. Kim, in *Proceedings of the Tau-Charm Factory Workshop*, SLAC, Stanford, CA, June 1989, SLAC-Report-343.
20. M. Bauer, B. Stech, and M. Wirbel, Z. Phys. **C34**, 101 (1987); M. Bauer and B. Stech, Phys. Lett. **152B**, 380 (1985).
21. B.Y. Blok and M.A. Shifman, Sov. J. Nucl. Phys. **45**, 135, 301, 522 (1987).
22. T. Inami and C.S. Lim, Prog. Theor. Phys. **65**, 297 (1981).
23. E. Ma and A. Pramudita, Phys. Rev. **D24**, 2476 (1981).
24. M. Selen, CLEO Collaboration, talk presented at *APS Spring Meeting*, Washington D.C., April 1994; J. Cumalet, these proceedings.
25. R. Ammar *et al.*, CLEO Collaboration, Phys. Rev. Lett. **71**, 674 (1993);
26. E. Golowich and S. Pakvasa, University of Massachusetts Report UNHEP-411 (1994); D. Atwood, B. Blok, and A. Soni, SLAC Report SLAC-PUB-6635 (1994).
27. G. Burdman, E. Golowich, J.L. Hewett, and S. Pakvasa, SLAC Report SLAC-PUB-6692 (1994).
28. A. Acker and S. Pakvasa, Mod. Phys. Lett. **A7**, 1219 (1992).
29. S. Davidson, D. Bailey, and B.A. Campbell, Z. Phys. **C61**, 613 (1994).
30. I.E. Stockdale, in *Proceedings of the Tau-Charm Factory Workshop*, SLAC, Stanford, CA, June 1989, SLAC-Report-343.
31. A. Datta, Z. Phys. **C27**, 515 (1985).
32. G. Burdman in *CHARM2000 Workshop*, Fermilab, June 1994; J. Donoghue *et al.*, Phys. Rev. **D33**, 179 (1986).
33. H. Georgi, Phys. Lett. **B297**, 353 (1992); T. Ohl *et al.*, Nucl. Phys. **B403**, 605 (1993).
34. K.S. Babu *et al.*, Phys. Lett. **B205**, 540 (1988); T.G. Rizzo, Int. J. Mod. Phys. **A4**, 5401 (1989).
35. J.L. Hewett, Phys. Rev. Lett. **70**, 1045 (1993); V. Barger, J.L. Hewett, and R.J.N. Phillips, Phys. Rev. **D41**, 3421 (1990).
36. S. Pakvasa and H. Sugawara, Phys. Lett. **73B**, 61 (1978); T.P. Cheng and M. Sher, Phys. Rev. **D35**, 3484 (1987); L. Hall and S. Weinberg, Phys. Rev. **D48**, 979 (1993).
37. I.I. Bigi, in *Proceedings of the Tau-Charm Factory Workshop*, SLAC, Stanford, CA, June 1989, SLAC-Report-343.
38. J.R. Fry and T. Ruf, in *Proceedings of the Marbella Workshop on the Tau-Charm Factory*, Marbella, Spain, June 1993.
39. F. Bucella *et al.*, Phys. Lett. **B302**, 319 (1993).
40. E. Golowich and G. Valencia, Phys. Rev. **D40**, 112 (1989); G. Burdman and J.F. Donoghue, Phys. Rev. **D45**, 187 (1992).
41. A. Le Yaouanc *et al.*, Phys. Lett. **B292**, 353 (1992).
42. S. Pakvasa, in in *CHARM2000 Workshop*, Fermilab, June 1994.

Fig. 1: Distribution[10] of difference between missing energy and momentum for Cabibbo allowed and suppressed semileptonic decays. The shaded regions correspond to the background levels assuming (a-b) lead-proportional tube calorimetry and (c-d) Cesium iodide crystal calorimetry.

Fig. 2: Missing mass distributions[19] for (a) $D^+ \to \mu^+\nu$, (b) $D_s^+ \to \mu^+\nu$, (c) $D^+ \to \tau^+\nu$ with $\tau \to \mu\bar{\nu}\nu$, and (d) $D_s^+ \to \tau^+\nu$ with $\tau \to e\bar{\nu}\nu$. The shaded regions correspond to the background levels.

Fig. 3: Reconstruction[3] of the decay $D_s \to \eta\pi^+\pi^+\pi^-$ with $\eta \to \pi^+\pi^-\pi^0$ and $\pi^0 \to \gamma\gamma$.

Fig. 4: Branching fraction for $D \to X + \ell^+\ell^-$ in the four generation SM as a function of the CKM mixing factor, with the solid, dashed, dotted, dash-dotted curve corresponding to $m_{b'} = 100, 200, 300, 400$ GeV, respectively.

Fig. 5: Δm_D in (a) the four generation SM with the same labeling as in Fig. 4, (b) in two-Higgs-doublet model II as a function of $\tan\beta$ with, from top to bottom, the solid, dashed, dotted, dash-dotted, solid curve representing $m_{H^\pm} = 50, 100, 250, 500, 1000\,\text{GeV}$. The solid horizontal line corresponds to the present experimental limit.

Fig. 6: (a) Constraints in the mass-mixing factor plane from Δm_D in the flavor changing Higgs model described in the text due to the tree-level process (solid curve) and the box diagram (dashed). (b) Constraints in the leptoquark coupling-mass plane from Δm_D.

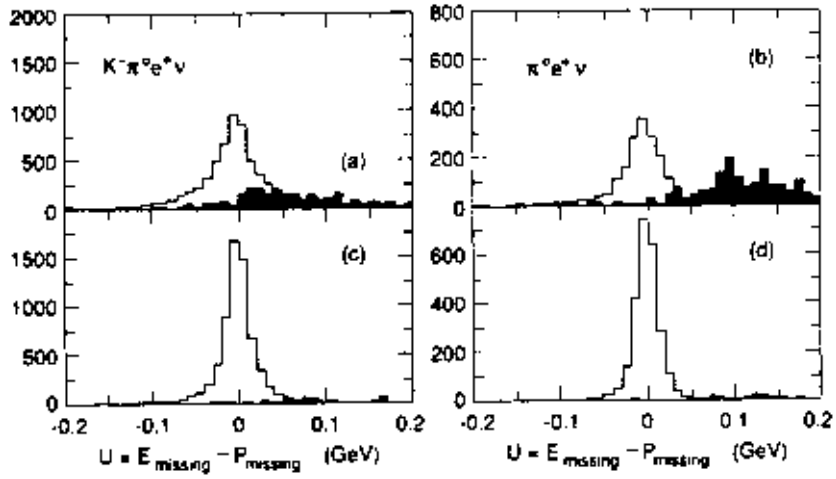
K⁻π°e⁺ν
(a)
(c)
π°e⁺ν
(b)
(d)
U = E_missing − P_missing (GeV)
U = E_missing − P_missing (GeV)

Fig. 1.

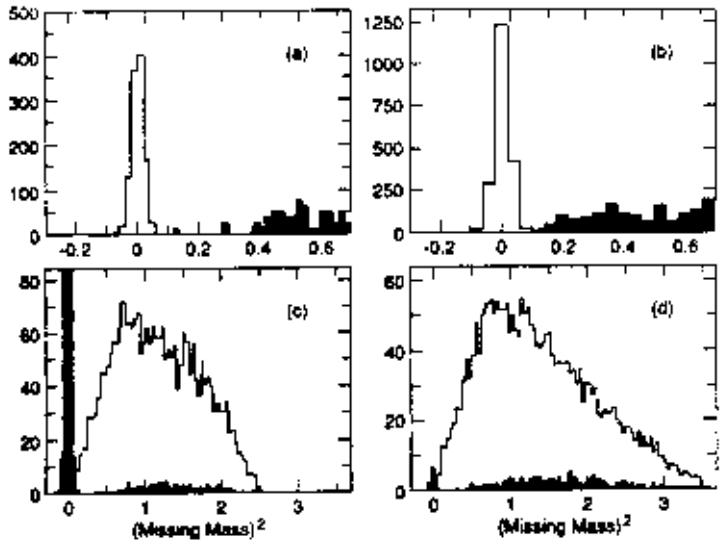
(a)
(b)
(c)
(d)
(Missing Mass)²
(Missing Mass)²

Fig. 2.

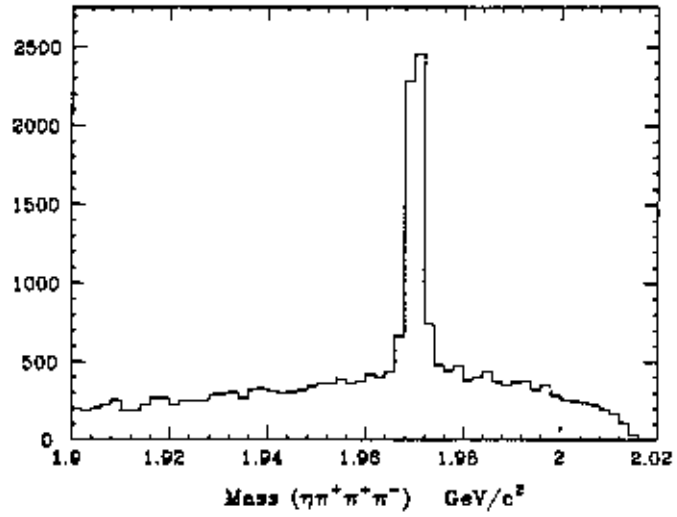
2500
2000
1500
1000
500
0
1.9
1.92
1.94
1.96
1.98
2
2.02
Mass ($\eta\pi^+\pi^+\pi^-$) GeV/c^2

Fig. 3.

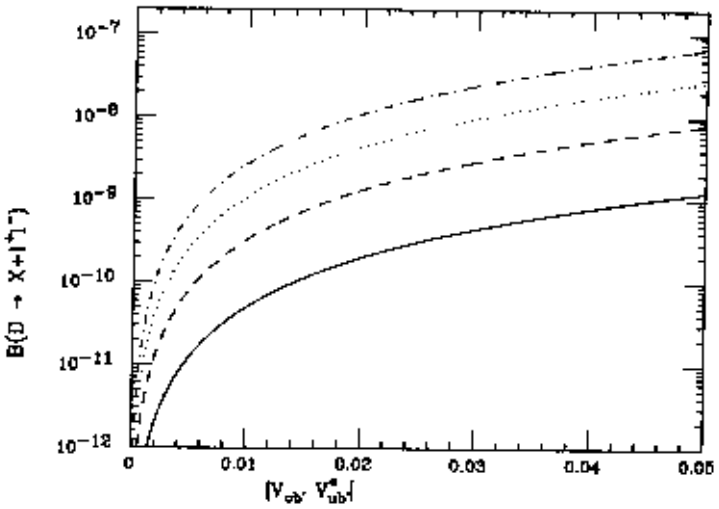
10^{-7}
10^{-8}
10^{-9}
10^{-10}
10^{-11}
10^{-12}
$B(D \to X+l^+l^-)$
0
0.01
0.02
0.03
0.04
0.05
$|V_{cb}\, V^*_{ub}|$

Fig. 4.

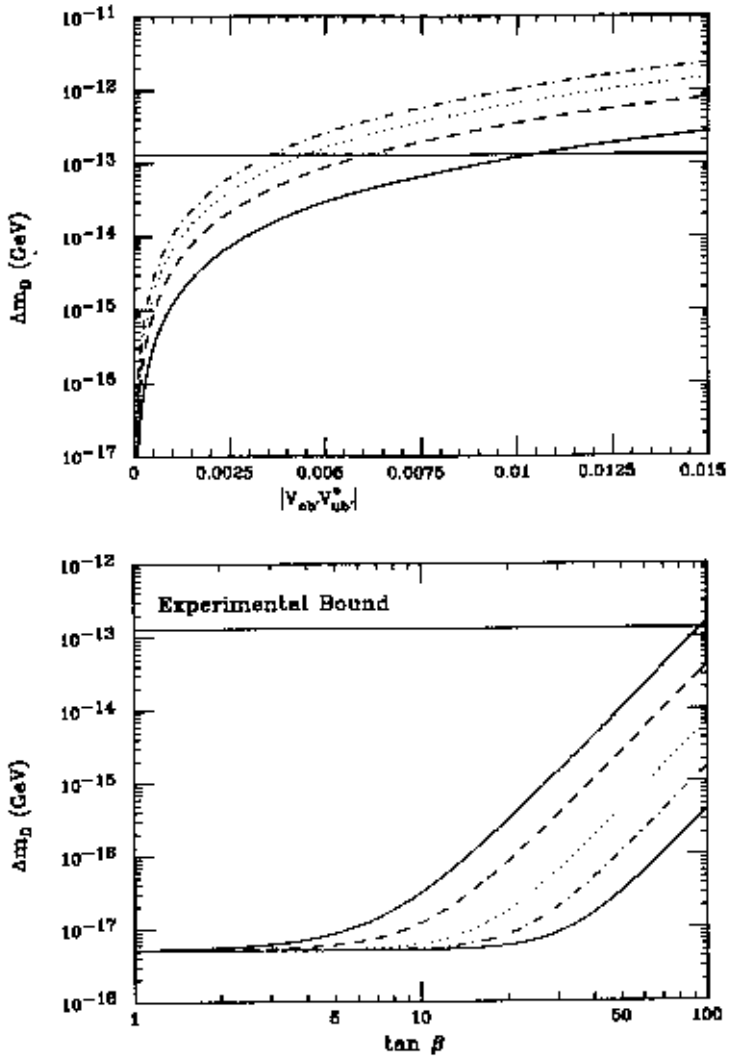
10^{-11}
10^{-12}
10^{-13}
10^{-14}
10^{-15}
10^{-16}
10^{-17}
Δm_B (GeV)
0
0.0025
0.005
0.0075
0.01
0.0125
0.015
$|V_{cb}V^*_{ub}|$
10^{-12}
10^{-13}
10^{-14}
10^{-15}
10^{-16}
10^{-17}
10^{-18}
Experimental Bound
Δm_B (GeV)
1
5
10
50
100
tan β

Fig. 5.

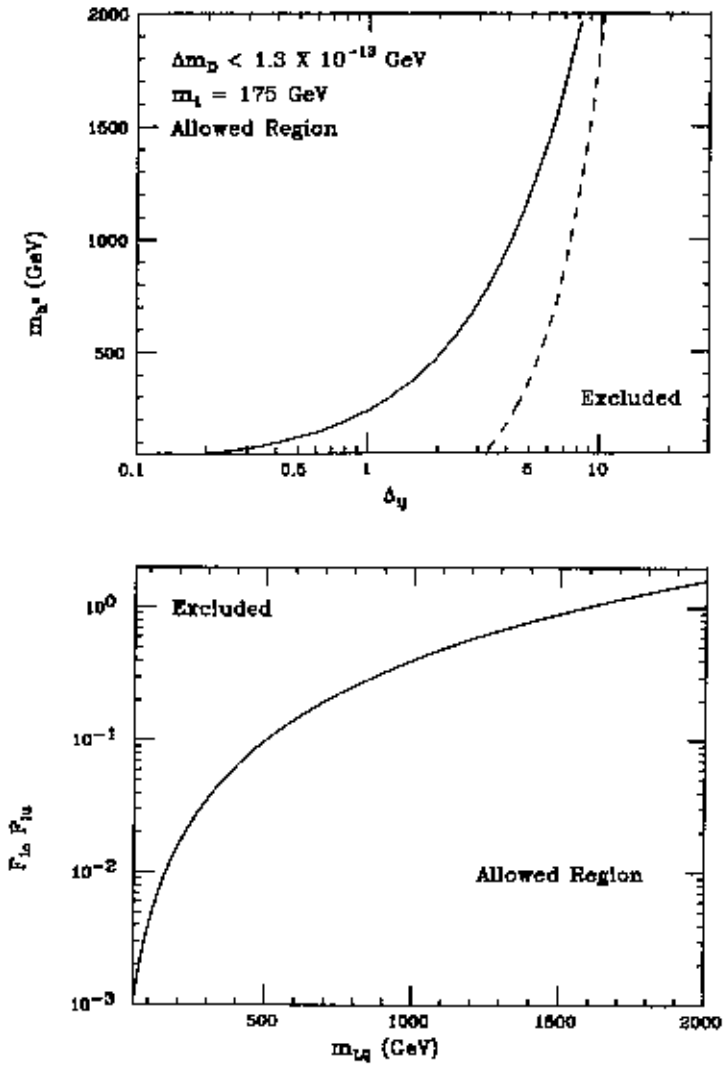
$\Delta m_D < 1.3 \times 10^{-13}$ GeV
m_t = 175 GeV
Allowed Region
Excluded
m_{h^0} (GeV)
δ_{ij}
2000
1500
1000
500
0.1
0.5
1
5
10
Excluded
Allowed Region
$F_{1i} F_{1i}$
m_{LQ} (GeV)
10^0
10^{-1}
10^{-2}
10^{-3}
500
1000
1500
2000

Fig. 6.